Letter

Entropic timescales of dynamic heterogeneity in supercooled liquid

Vinay Vaibhav[1,2,*] and Suman Dutta[3,†]

[1]*The Institute of Mathematical Sciences, CIT Campus, Taramani, Chennai 600113, India*

[2]*Department of Physics "A. Pontremoli", University of Milan, Via Celoria 16, 20133 Milan, Italy*

[3]*International Centre for Theoretical Sciences - Tata Institute of Fundamental Research Survey No 51, Hessaraghatta Hobli, Shivakote, Bangalore 560089, India*

(Received 27 September 2023; accepted 17 May 2024; published 6 June 2024)

Non-Gaussian displacement distributions are universal predictors of dynamic heterogeneity in slowly varying environments. Here, we explore heterogeneous dynamics in supercooled liquid using molecular dynamics simulations and show the efficiency of the relative-entropy based measure, negentropy, in quantifying dynamic heterogeneity over the widely used non-Gaussian parameter. Our analysis shows that the heterogeneity quantified by the negentropy is significantly different from the one obtained using the conventional moment-based definition that considers deviation from Gaussianity up to lower-order moments. We extract the timescales of dynamic heterogeneity using the two methods and show that the differential changes diverge as the system experiences strong intermittency near the glass transition. Further, we interpret the entropic timescales and discuss the general implications of our work.

DOI: 10.1103/PhysRevE.109.L062102

Introduction. Fickian theory of diffusion has been unquestionably successful for more than a century in analyzing particle-level dynamics in soft condensed matter that appear in different forms and shapes unless the system is intermittent or has widely separating timescales [1–23]. In metastable systems, such a route to diffusion becomes intermittent in the presence of complex energy landscapes, specifically, when a small magnitude of thermal fluctuation is not enough to supply the energy cost of achieving diffusion, overcoming the energy barriers [15,24]. For instance, molecular displacements deviate from their usual Gaussian form [3,5] in liquids approaching glass transition [25,26], showing slow heterogeneous density relaxation [27]. Such dramatic slowing down observed generically in a host of systems without any reproducible thermodynamic transition has remained a surprise even after decades of research [2,16,18]. Dynamic heterogeneity is the observed complex dynamics of particles in such temporally fluctuating environments in the presence of spatial degrees of heterogeneity, where both locally fast and slow relaxation processes coexist simultaneously [15,21,28–30].

Dynamic heterogeneity in the supercooled liquid has been affirmed with persisting non-Gaussian tails in the displacement distributions, even when the mean-squared displacement linearly increases with time [31,32]. Such a class of non-Gaussian diffusion has been explained as an effective dynamics in the presence of a diffusion spectrum where the dynamics is strongly influenced by the presence of cages, and diffusion is only restored upon cage breaking, making it distinct from the Fickian class of liquids [31,32]. The persistence of dynamic heterogeneity is thus debated for the presence of multiple timescales of relaxation and various ways of their determination [33–38]. It has also remained indecisive whether the onset of Fickian diffusion at all occurs in the finite time when a liquid approaches its glass transition [39–42].

Extracting the fundamental timescale of dynamic heterogeneity directly from the displacement distributions or the self-Van Hove function is more advantageous than obtaining it by other quantities which are either related to its moments or derivatives. Using the displacement distributions, it is possible to identify timescales of heterogeneity by finding the maximal non-Gaussianity using conventional measures that rely on moment-based relationships [43]. However, one hindrance of this method is that such moment ratios are primarily limited to lower-order moments, which raises natural question: How optimal are the non-Gaussianity-based estimation of complexity with respect to its determination by conventional techniques? This calls for newer directions in the precise identification of non-Gaussianity by informative approaches, akin to the information-theory-based optimizations that simplify multiscale and inverse problems in bioinformatics [44,45], explore material complexity [46–49], design metamaterials [50,51], develop data-driven decision making [52], predict catastrophes [53], innovate intelligent medical diagnostics [54,55], or help understand complex pathways of sensory response at synaptic levels [56].

Here, we explore dynamic heterogeneity in the supercooled liquid above the glass transition using molecular dynamics simulations in three dimensions. We examine the spatiotemporal dynamics in terms of the evolving probability distribution functions of the displacements at single particle level which are strongly heterogenous and non-Gaussian till

*vinay.vaibhav@unimi.it

†Corresponding author: suman.dutta@icts.res.in; Present Address: Simons Centre for the Study of Living Machines, National Centre for Biological Sciences–Tata Institute of Fundamental Research, Rajiv Gandhi Nagar, Kodigehalli, Bengaluru 560065, Karnataka.

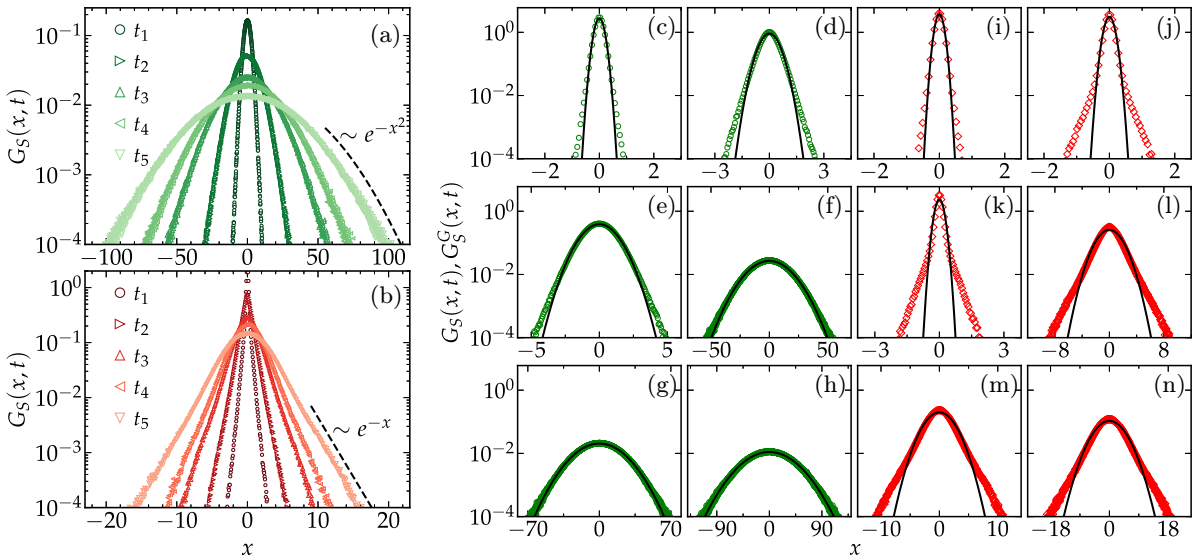

FIG. 1. [(a), (b)] Temporal evolution of the non-Gaussian displacement distributions, $G_S(x,t)$ vs x for two different T, (a) $T = 0.70$, (b) $T = 0.45$ for different t: $t_1 = 928.98, t_2 = 9527.62, t_3 = 39913.85, t_4 = 68300.79, t_5 = 139796.16$ with $x \in [X, Y, Z]$. Long time behavior of $G_S(x,t)$ at large x is Gaussian for $T = 0.70$ and exponential for $T = 0.45$. [(c)–(n)] Temporal evolution of the displacement distributions, $G_S(x,t)$ (open symbols) and respective reconstructed equal-time nearest Gaussians, $G_S^G(x,t)$ (black solid line) vs x for $T = 0.70$ [(c)–(h)] and $T = 0.45$ [(i)–(n)] for $t =$ 0.60 [(c), (i)], 21.62 [(d), (j)], 129.59 [(e), (k)], 27899.00 [(f), (l)], 47740.94 [(g), (m)], and 167210.14 [(h), (n)]. $G_S^G(x,t)$ are the optimal Gaussians with identical first two moments, the same as $G_S(x,t)$.

it diffuses at sufficiently long time. We quantify temporal intermittency in terms of non-Gaussianity extracted from the molecular displacements using the conventional moment-based descriptions and a relative entropy based non-Gaussian information that considers the statistical distance between the time-dependent displacement distribution and its equal-time nearest Gaussian trained from the original probability distribution functions. We extract and compare the identified timescales of optimal heterogeneity obtained from the two methods and show that they surprisingly differ in estimating microscopic heterogeneity, in particular when the situation is strongly intermittent at low temperatures. Further, we show that such a difference diverges when liquid becomes more viscous approaching the glass transition while they are comparable at relatively high temperatures, even within the supercooled regime. We correlate the two quantities and interpret the deviation.

Model. We simulate a well-studied model glass-forming system, popularly known as the Kob-Anderson 80:20 (A:B) binary mixture [57], in three dimensions at different temperatures T within the supercooled regime. The particles (each with unit mass) interact via the Lennard-Jones (LJ) pair potential with a cutoff at a distance R_c. Here, we use $N = 1000$ particles at a constant number density ($\rho = 1.20$) in a cubic box of length $L = 9.41$ and $R_c = 2.5$. All measurements are done in the LJ reduced unit (see Ref. [58] for model-related information). Independent molecular dynamics trajectories are generated using LAMMPS [59] under periodic boundary conditions with integration time step $\Delta t = 0.004$ at each of the different $T \in [0.43, 0.70]$.

Results. We track the particle trajectories and compute time-dependent probability distribution functions of particle displacements (also known as self-van Hove functions) which have been mapped in one dimension, x in time interval, t, $G_s(x,t) = \frac{1}{N}\sum_{i=1}^{N} \delta(x - (x_i(t) - x_i(0)))$ [60] by averaging over displacement distributions in all spatial dimensions obtained in different independent trajectories.

We show the time evolution of $G_S(x,t)$ for different t in Fig. 1 for two different values of T. At finite temperatures, $G_S(x,t)$ spreads with increasing t due to diffusion which we see here. For $T = 0.70$, it develops a non-Gaussian tail for intermediate times that reverts back to Gaussian at long times, suggesting that the dynamics is intermittent and heterogeneous even at relatively high temperatures, within the supercooled regime [Fig. 1(a)]. For $T = 0.45$, the heterogeneity is not only stronger but also its lifetime is prolonged as the non-Gaussian tail [$G_S(x,t) \sim \exp(-x/\lambda(t))$] with $\lambda(t) \sim \sqrt{t}$ persists for a very long time [Fig. 1(b)]. Such persistent exponential tails have been earlier reported in both simulations [10,25] and experiments [3,15,32].

In order to assess the degree of temporal heterogeneity in microscopic dynamics, we show the temporal evolution of $G_S(x,t)$ for various t for two different T in Figs. 1(c)–1(n) and compare it with the reconstructed equal-time nearest Gaussian distributions (see Ref. [61]), $G_S^G(x,t)$ that has first two moments the same as $G_S(x,t)$. This ensures that for a purely Gaussian distribution, $G_S^G(x,t) \to G_S(x,t)$ and $G_S^G(x,t) \neq G_S(x,t)$ when it is strictly non-Gaussian. We observe $G_S(x,t) \approx \delta(x)$ for $t = 0$, but the calculation of $G_S^G(x,t)$ will become more meaningful when $G_S(x,t)$ has some finite support at finite t. For $T = 0.70$, we observe that for very small t, the difference between $G_S(x,t)$ and $G_S^G(x,t)$ is not very significant [Fig. 1(c)]. The difference enhances with increasing t [Figs. 1(d) and 1(e)], where $G_S(x,t)$ is prominently non-Gaussian while for larger t, again $G_S(x,t)$ reverts back to Gaussian form with $G_S^G(x,t) \approx G_S(x,t)$ [Figs. 1(f)–1(h)],

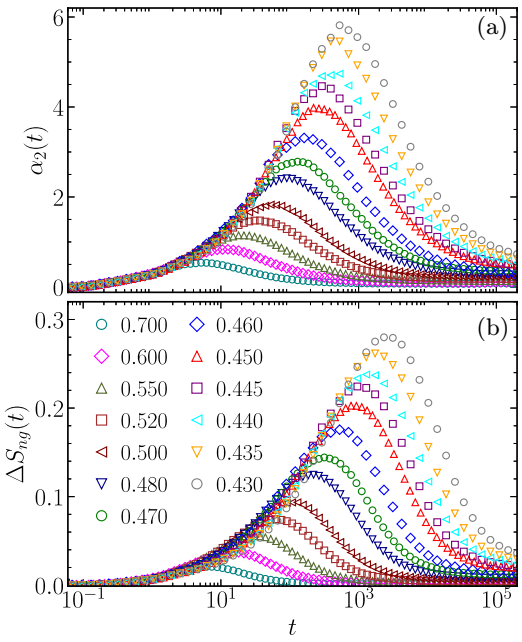

FIG. 2. Quantification of dynamic heterogeneity in terms of non-Gaussianity of $G_S(x,t)$ via (a) α_2, and (b) ΔS_{ng} vs t for different T as marked.

suggesting the onset of Fickian diffusion that is characterized by the presence of Gaussian displacement distribution and linear mean squared displacement [32].

The situation is surprisingly different for $T = 0.45$ which we show in Figs. 1(i)–1(n) and compare it with respective $G_S^G(x,t)$, as earlier. For small t, the distributions are highly spiked, centered at $x = 0$. Within the smaller intervals, $G_S(x,t) \approx G_S^G(x,t)$ [Fig. 1(i)] and smaller deviations from delta functions are mostly contributed by the lower-order moments. For larger t, as $G_S(x,t)$ broadens in x, more deviation could be seen from $G_S^G(x,t)$ in the form of exponential tail that grows with a significantly large proportion of displacements appearing beyond the support of the equal time nearest Gaussians [Figs. 1(j) and 1(k)], suggesting that the heterogeneity is maximally contributed by the higher-order moments. With increasing t [Figs. 1(l)–1(n)], the difference between $G_S(x,t)$ and $G_S^G(x,t)$ decreases yet it remains non-Gaussian within our observation time window.

Now we attempt to quantify the dynamic heterogeneity in terms of non-Gaussianity in $G_S(x,t)$ using conventional approaches that use lower order moment-based relationships. One such very simple quantification of non-Gaussianity that is widely available in the literature is based on the deviation of kurtosis from the square of second moment, defined as $\alpha_2(t) = \frac{\langle x^4(t)\rangle}{3\langle x^2(t)\rangle^2} - 1$ with $< x^n(t) >= \int dx\, x^n G_S(x,t)$, as in Ref. [1,3,57,62]. We show the dependence of α_2 with t for different T in Fig. 2(a). For $T = 0.70$, α_2 grows with increasing t till a peak is observed. After that, α_2 decreases for larger t. For smaller temperatures, the peak in α_2 shifts to larger t and the height of the peak grows. In all these cases, α_2 decreases monotonically after the peak. The timescale corresponding to the peak is generally identified as the characteristic timescale of dynamic heterogeneity. However, such quantification is fundamentally limited to fourth-order moments of $G_S(x,t)$. Figures 1(c)–1(n) suggest that the higher order moments may be associated with the larger degrees of heterogeneity for which we explore another quantification of non-Gaussianity that captures contributions of all order moments of $G_S(x,t)$ at a given time.

Non-Gaussianity in $G_S(x,t)$ is now analyzed using non-Gaussian information [61] that we developed following Ref. [63], originally proposed as negentropy. It uses the statistical distance between $G_S(x,t)$ and $G_S^G(x,t)$ to quantify $\Delta s_{ng}(t) = A\, D_{KL}(G_S(x,t)||G_S^G(x,t))$ where A is a constant. We further define, $\Delta S_{ng}(t)(= \Delta s_{ng}(t)/A) = -\int dx\, G_S(x,t) \log_e \frac{G_S^G(x,t)}{G_S(x,t)} = S_{ng}^G - S_{ng}$ when $G_S(x,t)$ has some finite support. Here, $S_{ng}(t) = -\int dx\, G_S(x,t) \log_e G_S(x,t)$ and $S_{ng}^G(t) = -\int dx\, G_S^G(x,t) \log_e G_S^G(x,t)$, and $D_{KL}(P||Q)$ is the Kullback-Leibler (KL) divergence [64] between two probability distribution functions, $P(x)$ and $Q(x)$. We show the time dependence of ΔS_{ng} for different T in Fig. 2(b). ΔS_{ng} shows nonmonotonic dependence on t, similar to α_2. For all these cases, ΔS_{ng} grows up to a peak and then decreases monotonically. Surprisingly, for every T, we observe that ΔS_{ng} still grows to higher values when α_2 has already reached the maximum. This suggests that the dynamic heterogeneity in $G_S(x,t)$ may not be completely captured in α_2 and the peak in α_2 may also not be a true representation of timescale of the underlying heterogeneity as it underestimates the contribution of the higher order moments in $G_S(x,t)$ because the information in α_2 is limited up to the fourth moment of the displacement distribution.

We compare the behavioural differences between α_2 and ΔS_{ng} in Fig. 3. In Fig. 3(a), we statistically correlate α_2 and ΔS_{ng} for the different cases of T. In all these cases, they form looplike shapes and the area covering the curve is larger for smaller T. We observe that the behavioral difference between α_2 and ΔS_{ng} grows when both have higher values, representing the maximal heterogeneity. The degree of such deviation significantly increases for decreasing T, suggesting strongly that the dynamic heterogeneity is underestimated by α_2 when $G_S(x,t)$ is maximally non-Gaussian. This is consistent with our earlier investigations [61] where we obtained similar loops in the case of a model supercooled liquid based on continuous time random walk (CTRW), suggesting that the underlying dynamic heterogeneity picture is qualitatively similar and the behavior of non-Gaussianity based quantifications remain universal under such slowly varying conditions.

We further extract the associated timescales corresponding to the peaks of α_2, τ_A and that of ΔS_{ng}, τ_S [see Fig. 2], and show its dependence on inverse of T in the inset of Fig. 3(b). Both τ_A and τ_S increase sharply for larger values of $1/T$. In all these cases, we observe that τ_S has higher values than that of τ_A. We finally correlate $\log_e \tau_A$ and $\log_e \tau_S$ in the main panel of Fig. 3(b). We fit the data of $\log_e \tau_S$ and $\log_e \tau_A$ and obtain $\log_e \tau_S \sim \beta_0 + \beta \log_e \tau_A$ with $\beta_0 \approx -0.411$, $\beta \approx 1.297$. This suggests that τ_S diverges from τ_A in a power-law ($\tau_S \sim \tau_A^{\beta}$) and such difference diverges with decreasing T. Further, we extract the height of the peak in ΔS_{ng}, $\Delta S_{ng}^P(T)(= \max_{t\in[0,\infty]} \Delta S_{ng}(t;T))$ and correlate it with the corresponding entropic timescale, τ_S. In the inset of Fig. 3(c), we show the dependence of $\log_e \tau_S$ on

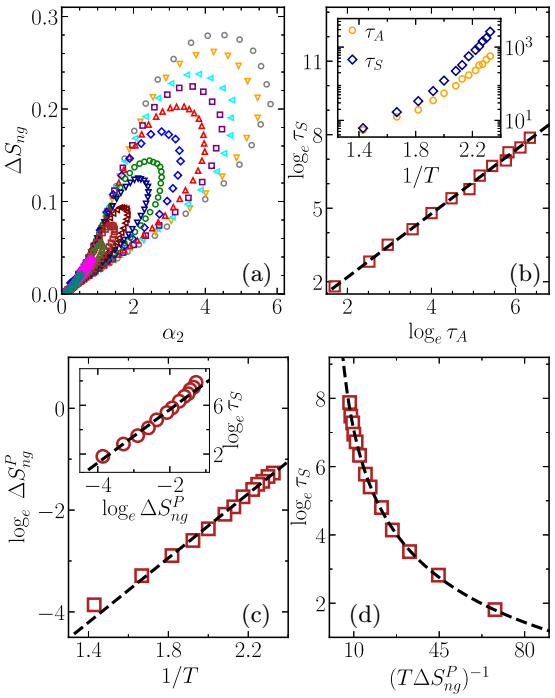

FIG. 3. (a) Correlating the non-Gaussian information, ΔS_{ng} with the non-Gaussian parameter, α_2 for different $T \in [0.43, 0.7]$ as marked in Fig. 2. (b) Inset: Temperature dependence of the timescales extracted corresponding to the peak of α_2, τ_A and ΔS_{ng}, τ_S. Main Panel: $\log_e \tau_S$ vs $\log_e \tau_A$. The dashed line shows a linear fit: $\log_e \tau_S \sim \beta_0 + \beta \log_e \tau_A$. (c) Dependence of $\log_e \Delta S^P_{ng}$ on $1/T$. Dashed line shows a fit with the form $\log_e \Delta S^P_{ng} \sim \nu_0 + \nu/T$. Inset: $\log_e \tau_S$ vs $\log_e \Delta S^P_{ng}$. The dashed line shows $\log_e \tau_S \sim \zeta_0 + \zeta \log_e \Delta S^P_{ng}$, (d) $\log_e \tau_S$ vs $(T\Delta S^P_{ng})^{-1}$. The dashed line shows $\log_e \tau_S \sim (T\Delta S^P_{ng})^{-\psi}$. See the text for the values of different fitting parameters.

$\log_e \Delta S^P_{ng}$. We observe that $\log_e \tau_S$ deviates from linear relationship with $\log_e \Delta S^P_{ng}$, which suggests that the dependence could not be fitted with simple power law in the low temperature regime. Further, $\log_e \Delta S^P_{ng}$ grows linearly with $1/T$ [Fig. 3(c)] when τ_S grows sharply with decreasing T [inset of Fig. 3(b)]. We fit the data as $\log_e \Delta S^P_{ng} \sim \nu_0 + \nu/T$ with $\nu_0 \approx -8.633$, $\nu \approx 3.162$. This suggests that the non-Gaussian information grows monotonically as T is lowered, accompanied with the sharp increase in τ_S, as the system approaches the state of dynamic arrest. Hence, ΔS^P_{ng} becomes a natural characteristic indicator of the degree of heterogeneity at a given T. Thus, with decreasing T, the system explores increasingly stronger intermittent environment and dynamically heterogeneous states with larger non-Gaussian information, ΔS^P_{ng}, capturing the absolute entropic distance between the state of characteristic heterogeneity from its nearest diffusive route. Hence, the term $T\Delta S^P_{ng}$ can be considered as an energy term associated with the heterogeneity that competes with the diffusion in overcoming the dynamic heterogeneity at a given T. So, we correlate the entropic timescale, τ_S with $1/(T\Delta S^P_{ng})$ and observe that τ_S grows and shows a sharp rise with decreasing $1/(T\Delta S^P_{ng})$ [Fig. 3(d)]. Our data follows $\log_e \tau_S \sim \eta_0 + \eta(T\Delta S^P_{ng})^{-\psi}$ with $\eta_0 \approx -8.551$, $\eta \approx 25.630$, $\psi \approx -0.215$. Using the form of ΔS^P_{ng} as suggested by the data shown in Fig. 3(c), one can obtain $\log_e \tau_S \sim \eta[T \exp(\nu_0 + \nu/T)]^{-\psi}$ whose temperature dependence is essentially given by $\log_e \tau_S \sim T^{-\psi} \exp(-\nu\psi/T)$. At sufficiently low temperatures, it also suggests that the growth of $\log_e \tau_S$ is likely to be dominated primarily by the factor $\sim \exp(-\nu\psi/T)$ for $\nu > 0, \psi < 0$, which qualitatively explains the nature of growth of τ_S with decreasing T, as well as for the cases when $\tau_S \sim O(1)$ at relatively high T within the supercooled regime, as indicated by the data shown [in the inset of Fig. 3(b)]. The rapid rise of τ_S is due to the presence of strong intermittency, for which achieving diffusion becomes increasingly difficult overcoming the barriers of heterogeneity, for the exploration within the rough energy landscapes at low temperatures.

Discussion. These results align with our theoretical predictions of the entropic timescales of dynamic heterogeneity in a model supercooled liquid [61] where the development of intermittent non-Gaussian tail was modeled using the Montroll-Weiss CTRW framework, considering complex hopping of particles within the mobile and immobile regions and jumps from one region to another [65]. The persistence of such vibrations and jumps within these regions overall controls the nature of intermittency and its lifetime [25,26]. Such intermittent non-Gaussian tails were inferred as a convolution process of cooperative diffusion, known as the Brownian yet non-Gaussian diffusion [32,66]. Supportive literature [21,22,67–70] shows that the diffusion spectrum obtained upon the deconvolution of the non-Gaussian displacement distribution validates the physical picture of dynamic heterogeneity which considers the simultaneous presence of slow and fast regions within the system [30,36–38]. Such heterogeneity exhibits anomalous spatiotemporal fluctuations that have all order information [71]. Therefore, to estimate the dynamic heterogeneity effectively, consideration of all order moments is advantageous. Gaussianity reverts when the Fickian diffusion sets in and the dynamics follow the central limit theorem, marking the onset of diffusion. However, extraction of this timescale becomes increasingly difficult when the dynamics becomes strongly heterogeneous, and non-Gaussianity in the displacement distributions persists for very long times. Our analysis also affirms that τ_S grows with increasing τ_A in a power law which can be further tested using CTRW models [25,26] or using mode coupling theory [72]. The sharp increase of ΔS^P_{ng} with decreasing T is due to diverging dynamic heterogeneity that also leads to a sharp increase in entropic timescale as the system approaches the state of dynamic arrest. At such close vicinity of the glass transition, it should also be interesting to compare different timescales of heterogeneity, that appear due to dynamical slowing down and low-probable spatiotemporal fluctuations responsible for cage breaking [33–38]. Whether the non-Gaussian-information has any connection with the predictability [46], structural relaxation [73], configurational entropy [74], or nonequilibrium free energy [75] needs further investigation.

Conclusions. We quantify the timescales of dynamic heterogeneity in supercooled liquids using the conventional non-

Gaussian parameter and the non-Gaussian information. We show that the entropic timescales are significantly different and diverge from those obtained using the non-Gaussian parameter. This difference arises because the moment-based definitions are limited up to the fourth order, while the information-theoretic quantification takes into account all order moments. Although several other moment-based definitions are available [62,76], it is always challenging to estimate timescales using them, as the computation of higher-order moments can be increasingly noisy or unreliable without the quality data. On the other hand, our framework is easy to implement and extract heterogeneity optimally. This makes the information theoretic framework scientifically robust in quantifying non-Gaussianity in practical situations, also in a more general context, in out-of-equilibrium systems in identifying or predicting novel crossover or transition where small fluctuations lead to catastrophic changes, or differentiate phases or states of matter [71,77].

Acknowledgments. We thank L. Berthier, S. Bose, P. Chaudhuri, C. Dasgupta, J. Horbach, S. Karmakar, S. K. Nandi, M. S. Shell, and A. Zaccone for insightful discussions. V.V. gratefully acknowledges funding from the European Union through Horizon Europe ERC Grant No. 101043968 "Multimech." S.D. acknowledges support of the Department of Atomic Energy, Government of India, under Project No. RTI4001. We acknowledge HPC facilities at IMSc, ICTS-TIFR and supporting grants, ICTS/eiosm2018/08, ICTS/ISPCM2023/02. We also thank D. Bagchi and S. Sikdar for sharing data.

[1] W. Kob, C. Donati, S. J. Plimpton, P. H. Poole, and S. C. Glotzer, Phys. Rev. Lett. **79**, 2827 (1997).
[2] M. D. Ediger, Annu. Rev. Phys. Chem. **51**, 99 (2000).
[3] W. K. Kegel and A. van Blaaderen, Science **287**, 290 (2000).
[4] E. R. Weeks, J. C. Crocker, A. C. Levitt, A. Schofield, and D. A. Weitz, Science **287**, 627 (2000).
[5] Y. Gao and M. L. Kilfoil, Phys. Rev. Lett. **99**, 078301 (2007).
[6] R. Richert, J. Phys.: Condens. Matter **14**, R703 (2002).
[7] E. Bertin, J.-P. Bouchaud, and F. Lequeux, Phys. Rev. Lett. **95**, 015702 (2005).
[8] N. Lačević, F. W. Starr, T. B. Schrøder, and S. C. Glotzer, J. Chem. Phys. **119**, 7372 (2003).
[9] H. C. Andersen, Proc. Natl. Acad. Sci. **102**, 6686 (2005).
[10] M. S. Shell, P. G. Debenedetti, and F. H. Stillinger, J. Phys.: Condens. Matter **17**, S4035 (2005).
[11] E. Flenner and G. Szamel, Phys. Rev. Lett. **105**, 217801 (2010).
[12] J. P. Garrahan, Proc. Natl. Acad. Sci. **108**, 4701 (2011).
[13] K. Martens, L. Bocquet, and J-L. Barrat, Phys. Rev. Lett. **106**, 156001 (2011).
[14] L. Berthier, Physics **4**, 42 (2011).
[15] L. Berthier, G. Biroli, J.-P. Bouchaud, L. Cipelletti, and W. van Saarloos, *Dynamical Heterogeneities in Glasses, Colloids, and Granular Media* (Oxford University Press, New York, 2011), Vol. 150.
[16] L. Berthier and G. Biroli, Rev. Mod. Phys. **83**, 587 (2011).
[17] E.-M. Schötz, M. Lanio, J. A. Talbot, and M. L. Manning, J. R. Soc., Interface **10**, 20130726 (2013).
[18] S. Karmakar, C. Dasgupta, and S. Sastry, Annu. Rev. Condens. Matter Phys. **5**, 255 (2014).
[19] E. Flenner, H. Staley, and G. Szamel, Phys. Rev. Lett. **112**, 097801 (2014).
[20] W. Zhang, J. F. Douglas, and F. W. Starr, J. Chem. Phys **146**, 203310 (2017).
[21] B. P. Bhowmik, I. Tah, and S. Karmakar, Phys. Rev. E **98**, 022122 (2018).
[22] R. Das, C. Dasgupta, and S. Karmakar, Front. Phys. **8**, 210 (2020).
[23] P. Pareek, M. Adhikari, C. Dasgupta, and S. K. Nandi, J. Chem. Phys. **159**, 174503 (2023).
[24] A. Heuer, J. Phys.: Condens. Matter **20**, 373101 (2008).
[25] P. Chaudhuri, L. Berthier, and W. Kob, Phys. Rev. Lett. **99**, 060604 (2007).
[26] P. Chaudhuri, Y. Gao, L. Berthier, M. Kilfoil, and W. Kob, J. Phys.: Condens. Matter **20**, 244126 (2008).
[27] B. Vorselaars, A. V. Lyulin, K. Karatasos, and M. A. J. Michels, Phys. Rev. E **75**, 011504 (2007).
[28] S. Karmakar, C. Dasgupta, and S. Sastry, Phys. Rev. Lett. **105**, 015701 (2010).
[29] G. Gradenigo, E. Bertin, and G. Biroli, Phys. Rev. E **93**, 060105(R) (2016).
[30] S. Dutta, Chem. Phys. **522**, 256 (2019).
[31] B. Wang, S. M. Anthony, S. C. Bae, and S. Granick, Proc. Natl. Acad. Sci. **106**, 15160 (2009).
[32] B. Wang, J. Kuo, S. C. Bae, and S. Granick, Nat. Mater. **11**, 481 (2012).
[33] S. C. Glotzer, V. N. Novikov, and T. B. Schrøder, J. Chem. Phys. **112**, 509 (2000).
[34] S. Karmakar, C. Dasgupta, and S. Sastry, Proc. Natl. Acad. Sci. **106**, 3675 (2009).
[35] E. Flenner and G. Szamel, Phys. Rev. E **72**, 011205 (2005).
[36] P. Das and S. Sastry, J. Non-Cryst. Solids **14**, 100098 (2022).
[37] T. Kawasaki and K. Kim, Sci. Adv. **3**, e1700399 (2017).
[38] T. Kawasaki and K. Kim, J. Stat. Mech. (2019) 084004.
[39] L. Berthier, E. Flenner, and G. Szamel, Phys. Rev. Lett. **131**, 119801 (2023).
[40] F. Rusciano, R. Pastore, and F. Greco, Phys. Rev. Lett. **131**, 119802 (2023).
[41] E. Barkai and S. Burov, Phys. Rev. Lett. **124**, 060603 (2020).
[42] F. Rusciano, R. Pastore, and F. Greco, Phys. Rev. Lett. **128**, 168001 (2022).
[43] K. Binder and W. Kob, *Glassy Materials and Disordered Solids: An Introduction to Their Statistical Mechanics* (World Scientific, Singapore, 2011).
[44] M. S. Shell, Coarse-graining with the relative entropy, in *Advances in Chemical Physics*, Vol. 161, edited by S. A. Rice and A. R. Dinner (John Wiley, Hoboken, 2016).
[45] M. Gabrié, A. Manoel, C. Luneau, J. Barbier, N. Macris, F. Krzakala, and L. Zdeborová, J. Stat. Mech. (2019) 124014.
[46] R. L. Jack, A. J. Dunleavy, and C. P. Royall, Phys. Rev. Lett. **113**, 095703 (2014).

[47] E. D. Cubuk, S. S. Schoenholz, J. M. Rieser, B. D. Malone, J. Rottler, D. J. Durian, E. Kaxiras, and A. J. Liu, Phys. Rev. Lett. **114**, 108001 (2015).
[48] V. Bapst, T. Keck, A. Grabska-Barwińska, C. Donner, E. D. Cubuk, S. S. Schoenholz, A. Obika, A. W. Nelson, T. Back, D. Hassabis, and P. Kohli, Nat. Phys. **16**, 448 (2020).
[49] G. Jung, G. Biroli, and L. Berthier, Phys. Rev. Lett. **130**, 238202 (2023).
[50] L. J. Kwakernaak and M. van Hecke, Phys. Rev. Lett. **130**, 268204 (2023).
[51] K. Bertoldi, V. Vitelli, J. Christensen, and M. van Hecke, Nat. Rev. Mater. **2**, 17066 (2017).
[52] S. K. Stavroglou, A. A. Pantelous, and H. E. Stanley, Proc. Natl. Acad. Sci. USA **115**, 867 (2018).
[53] S. K. Stavroglou, A. A. Pantelous, H. E. Stanley, and K. M. Zuev, Proc. Natl. Acad. Sci. USA **116**, 10646 (2019).
[54] P. Washington, N. Park, P. Srivastava, C. Voss, A. Kline, M. Varma, Q. Tariq, H. Kalantarian, J. Schwartz, R. Patnaik, B. Chrisman, N. Stockham, K. Paskov, N. Haber, and D. P. Wall, Biol. Psychiatry. Cogn. Neurosci. Neuroimaging. **5**, 759 (2020).
[55] J. Lee and D. M. Maslove, BMC. Med. Inform. Decis. Mak. **15**, 59 (2015).
[56] J. D. Victor, Biol. Theory. **1**, 302 (2006).
[57] W. Kob and H. C. Andersen, Phys. Rev. E **51**, 4626 (1995).
[58] V. Vaibhav, J. Horbach, and P. Chaudhuri, Phys. Rev. E **101**, 022605 (2020).
[59] S. Plimpton, J. Comput. Phys. **117**, 1 (1995).
[60] L. Van Hove, Phys. Rev. **95**, 249 (1954).
[61] R. Dandekar, S. Bose, and S. Dutta, Europhys. Lett. **131**, 18002 (2020).
[62] J. Horbach, W. Kob, and K. Binder, Philos. Mag. B **77**, 297 (1998).
[63] J. S. Ivan, M. S. Kumar, and R. Simon, Quantum Inf. Process. **11**, 853 (2012).
[64] S. Kullback and R. A. Leibler, Ann. Math. Stat. **22**, 79 (1951).
[65] J. S. Langer and S. Mukhopadhyay, Phys. Rev. E **77**, 061505 (2008).
[66] A. V. Chechkin, F. Seno, R. Metzler, and I. M. Sokolov, Phys. Rev. X **7**, 021002 (2017).
[67] S. Dutta and J. Chakrabarti, Europhys. Lett. **116**, 38001 (2016).
[68] M. V. Chubynsky and G. W. Slater, Phys. Rev. Lett. **113**, 098302 (2014).
[69] V. Sposini, A. Chechkin, and R. Metzler, J. Phys. A: Math. Theor. **52**, 04LT01 (2019).
[70] R. Jain and K. L. Sebastian, J. Phys. Chem. B **120**, 9215 (2016).
[71] E. Lemaitre, I. M. Sokolov, R. Metzler, and A. V. Chechkin, New J. Phys. **25**, 013010 (2023).
[72] S.-H. Chong, Phys. Rev. E **78**, 041501 (2008).
[73] A. J. Dunleavy, K. Wiesner, R. Yamamoto, and C. P. Royall, Nat. Commun. **6**, 6089 (2015).
[74] F. W. Starr, J. F. Douglas, and S. Sastry, J. Chem. Phys. **138**, 12A541 (2013).
[75] J. M. R. Parrondo, J. M. Horowitz, and T. Sagawa, Nat. Phys. **11**, 131 (2015).
[76] G. Szamel and E. Flenner, Phys. Rev. E **73**, 011504 (2006).
[77] X. Zheng, B. ten Hagen, A. Kaiser, M. Wu, H. Cui, Z. Silber-Li, and H. Löwen, Phys. Rev. E **88**, 032304 (2013).